molecules

MDPI

Article

Naphthenic Acids Removal from Model Transformer Oil by Diethylamine Modified Resins

Yan Wang [1], Peng Dou [2], Xiaofeng You [1], Qing Liu [1,*], Zhaoyang Fei [1], Xian Chen [1], Zhuxiu Zhang [1], Jihai Tang [1], Mifen Cui [1] and Xu Qiao [1,3,*]

[1] State Key Laboratory of Materials−Oriented Chemical Engineering, College of Chemical Engineering, Nanjing Tech University, Nanjing 211816, China
[2] Jiangsu Frontier Electric Technology Co., Ltd., Nanjing 211102, China
[3] Jiangsu National Synergetic Innovation Center for Advanced Materials (SICAM), Nanjing 211800, China
* Correspondence: qing_liu@njtech.edu.cn (Q.L.); qct@njtech.edu.cn (X.Q.); Tel./Fax: +86-(25)-83587168 (Q.L.); +86-(25)-8317229 (X.Q.)

Abstract: Resins have enormous potential in the removal of naphthenic acids (NAs) from transformer oil due to their rich porosity and high mechanical and diversified functionality, whereas their poor adsorption capacity limits application. In this work, the polystyrene–diethylamine resin (PS−DEA−x) was prepared by grafting diethylamine (DEA) onto chloromethylated polystyrene (PS−Cl) resin to efficiently adsorb cyclopentane carboxylic acid from transformer oil for the first time. The characterization analysis results indicated that amine contents were significantly enhanced with the increase in DEA. Particularly, resin with a molar ratio of 1:5 depending on chloromethyl to DEA (PS−DEA−5) exhibited the highest amine contents and efficient adsorption of cyclopentane carboxylic acid (static adsorption capacity up to 110.0 mg/g), which was about 5 times higher than that of the pristine PS−Cl. The thermodynamic and kinetic studies showed that the adsorption behaviors could be well fitted to the Langmuir isotherm equation and pseudo−second−order rate equation. Moreover, it was found that 1 g of the PS−DEA−5 can decontaminate about 760 mL transformer oil to meet reuse standards by a continuous stream, indicating its potential application in industry.

Keywords: resin; diethylamine; chemical modification; cyclopentane carboxylic acid; transformer oil purification

Citation: Wang, Y.; Dou, P.; You, X.; Liu, Q.; Fei, Z.; Chen, X.; Zhang, Z.; Tang, J.; Cui, M.; Qiao, X. Naphthenic Acids Removal from Model Transformer Oil by Diethylamine Modified Resins. *Molecules* **2023**, *28*, 2444. https://doi.org/10.3390/molecules28062444

Academic Editor: Yan'an Gao

Received: 28 November 2022
Revised: 27 February 2023
Accepted: 1 March 2023
Published: 7 March 2023

1. Introduction

Transformer oil is an essential insulating medium for power transmission and transformation equipment in a power system [1,2]. However, transformer oil will produce corrosive naphthenic acids (NAs) in the process of use, which causes a severe threat to the transformer [3–6]. Hence, the effective removal of NAs from transformer oil is essential. In recent years, numerous methods have been carried out to treat transformer oil containing NAs [7–9]. Among these methods, adsorption is gradually perceived as the sensible solution for NAs removal due to its simplicity, economic feasibility, and high efficiency [10–12].

NAs, a kind of weak acid, are a mixture of alicyclic carboxylic acid and saturated aliphatic acid [13,14]. More recently, in order to improve the adsorption capacity towards NAs, amine groups have typically been introduced into adsorbents because they can interact with NAs through acid–base interaction, hydrogen bonding, and electrostatic interaction [15,16]. For instance, Hojatallah et al. [17] modified commercial activated carbon (AC) and petroleum activated carbon (PAC) through the amination process. They pointed out that the introduced amine groups can interact with the NAs and the adsorption process can be controlled by chemisorption. Galina et al. [12] prepared amino−functionalized silica−coated iron oxide (Fe_3O_4/SiO_2 NH_2/C_{18}) magnetic nanoparticles, and they found

that Fe_3O_4/SiO_2 NH_2/C_{18} had a 2.7 times higher adsorption capacity compared to the unmodified silica−coated (Fe_3O_4/SiO_2) nanoparticles toward 4−heptylbenzoic acid from octane. For now, most studies concerning NA removal still concentrate on the water phase, while only a few study the extraction of NAs from the oil phase. Additionally, practical applications of these adsorbents are limited because of high cost and synthesis difficulty, and powdered adsorbents are hard to separate from oil [18,19]. Hence, it is necessary to design a suitable adsorbent for the adsorption of NAs from transformer oil.

In recent years, resins have drawn significant attention in the removal of NAs from transformer oil, since they display high specific surface area, strong mechanical strength, tunable porous texture, and easy separation. Debashish et al. [15] studied commercial weak and strong anion−exchange resins. They found that the weakly anionic ion−exchange resins with a weak tertiary amine group had higher adsorption capacity towards NAs from petroleum oil than the strong anion−exchange resins, and the rate of adsorption of NAs using the ion−exchange resin was governed by the intraparticle diffusion processes. Macroporous chloromethylated polystyrene (PS−Cl) is an ideal polymeric matrix with stable mechanical properties. The active chloromethyl group in PS−Cl can be easily converted into a number of new functional groups via special reactions [20]. Aside from that, the PS−Cl surface is not susceptible to shed fragments nor easily separated, which will not have a negative impact on the physical and chemical properties of transformer oil after adsorption [21]. Therefore, in order to obtain high adsorption capacity for NAs, chemical modification of PS−Cl is adopted by introducing diethylamine (DEA) containing a tertiary amine group onto the PS−Cl [22–24].

Based on the above discussion, we prepared a series of resins with different amine contents using DEA−modified PS−Cl to reinforce NA adsorption in transformer oil. Various characteristic analysis methods were used to verify the successful introduction of DEA in PS−Cl. Particularly, the adsorption process was described by kinetic, thermodynamic, and dynamic adsorption studies. Since the real system is a complex mixture of chemical species, the adopted approach to promote a better comprehension of the phenomenon was to study model systems composed of cyclopentane carboxylic acid with transformer oil.

2. Results and Discussion

2.1. Characterization

The FT−IR spectra of the synthesized resin were investigated to better confirm the chemical structures, as shown in Figure 1. The FT−IR spectra presented in Figure 1 indicated that successful amination reactions happened between PS−Cl and DEA. It was obvious that the strong vibrations at 1265 cm^{-1} identified as $-CH_2Cl$ groups of PS−Cl were significantly weakened after the amination reaction [25,26]. This phenomenon may result from the reaction between the amine group of the DEA and the $-CH_2Cl$ in the PS−Cl, leading to the gradual decrease in chloromethyl groups. Meanwhile, all typical peaks of DEA can be observed in the PS−DEA−x. The new peaks at 2975 cm^{-1} and 1370 cm^{-1} were found due to the stretching and bending vibration of $-CH_3$ in DEA, while the peak at 1200 cm^{-1} was ascribed to the stretching vibration of C−N in DEA [27]. These results showed that DEA was successfully grafted into PS−DEA−x. At the same time, this result was further corroborated by the EA, as shown in Table 1. The nitrogen content of the obtained six resins was measured to be 0.06%, 3.16%, 4.51%, 5.59%, 5.96% and 6.04% (wt%), which demonstrated that DEA was successfully grafted into the PS−Cl.

The TG of the PS−DEA−x is shown in Figure 2. The initial mass loss of 25% from 200 to 350 °C of PS−Cl was attributed to decomposition of the $-CH_2Cl$ [28], which was significantly reduced with the increase in the percentage of DEA in PS−DEA−x. When the temperature exceeded 350 °C, the weight loss of all the resins was above 80% owing to the fracture of the PS−DEA−x skeleton [29]. These results indicated that DEA was successfully grafted into the framework of PS−Cl.

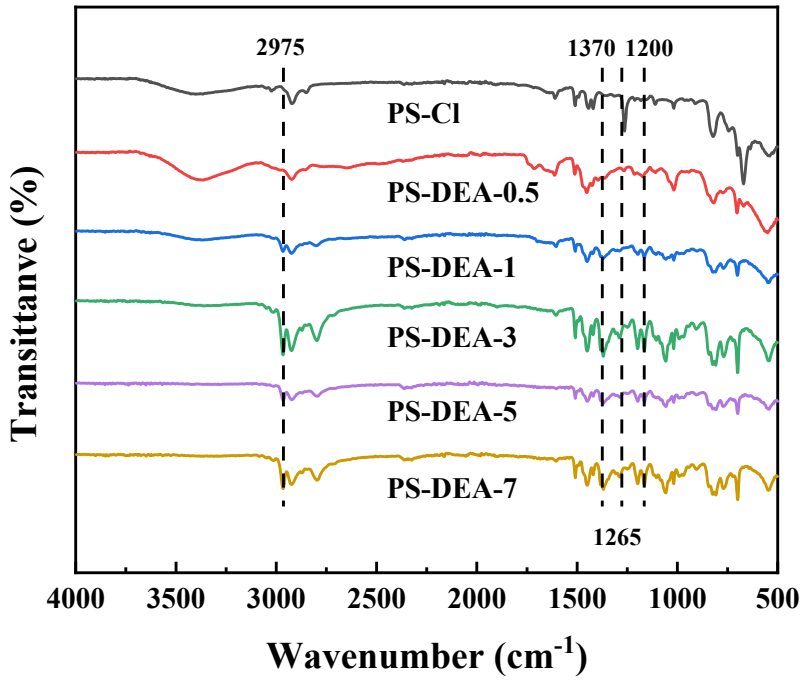

Figure 1. FT−IR spectra of PS−DEA−x.

Table 1. Element contents in different PS−DEA−x.

Samples	C (%)	N (%)	H (%)
PS−Cl	54.46	0.06	6.43
PS−DEA−0.5	63.64	3.16	7.89
PS−DEA−1	72.99	4.51	8.50
PS−DEA−3	81.42	5.59	9.15
PS−DEA−5	82.37	5.96	9.51
PS−DEA−7	82.45	6.04	9.40

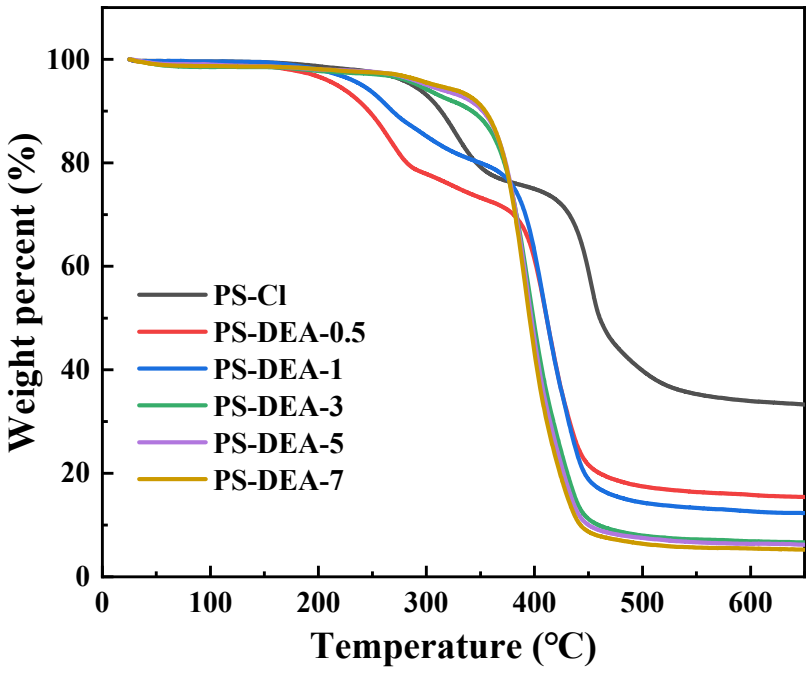

Figure 2. TG analytical curves of PS−DEA−x.

Figure 3 and Table 2 present the data derived from N_2 adsorption–desorption analysis to evaluate the textural properties of PS−DEA−x. The N_2 adsorption isotherms of PS−Cl and PS−DEA−x were assigned to Type IV, and the hysteresis ring of PS−DEA−x belongs to H3 (Figure 3a), demonstrating that the synthesized PS−DEA−x have mesoporous structure. As seen from Table 2, compared with the pristine PS−Cl, the BET surface areas and pore volume of the resins exhibited a slight decrease after the amination reaction. It can be concluded that the reduced pore volume after DEA graft was attributed to the DEA grafting in the pores [29]. However, with the continuous addition of DEA, the chloromethyl group in the pores gradually decreased and the DEA was unable to react with the chloromethyl group; thus, the BET surface areas and pore volume could not continue to decrease. These results indicated that DEA was successfully grafted into the pores of PS−Cl and that PS−DEA−x still maintains a mesoporous structure after DEA grafting.

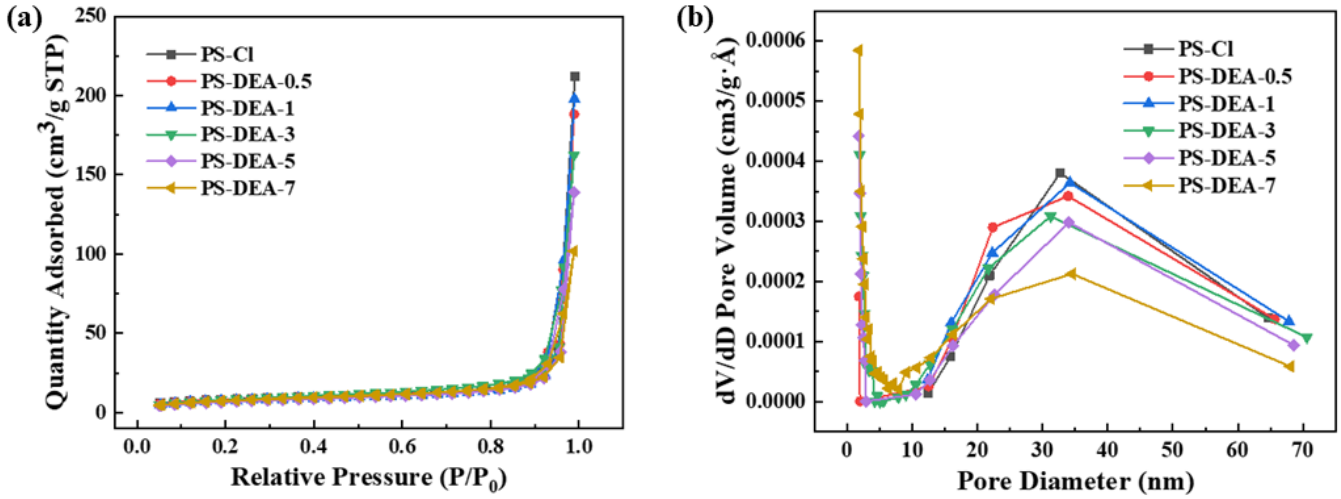

Figure 3. (**a**) N_2 ad−desorption curves and (**b**) pore size distribution curves of PS−DEA−x.

Table 2. Specific surface area and total pore volume of PS−DEA−x.

Samples	S_{BET} (m^2/g)	V_P (cm^3/g)
PS−Cl	32	0.45
PS−DEA−0.5	31	0.40
PS−DEA−1	30	0.39
PS−DEA−3	27	0.37
PS−DEA−5	26	0.36
PS−DEA−7	25	0.33

The surface morphology of the resin before and after modification was studied via SEM (Figure 4). It can be found that the surface of PS−Cl was relatively smooth, while the surface of DEA−modified resin showed obvious cracks, which may be imputed to the grafting of DEA on the surface of the resin. The cracks on the surface of the modified resin make it different from pristine PS−Cl and were conducive to the diffusion of pollutants in the transformer oil into the resin, further revealing the partial grafting of the DEA on the surface of the resin [30].

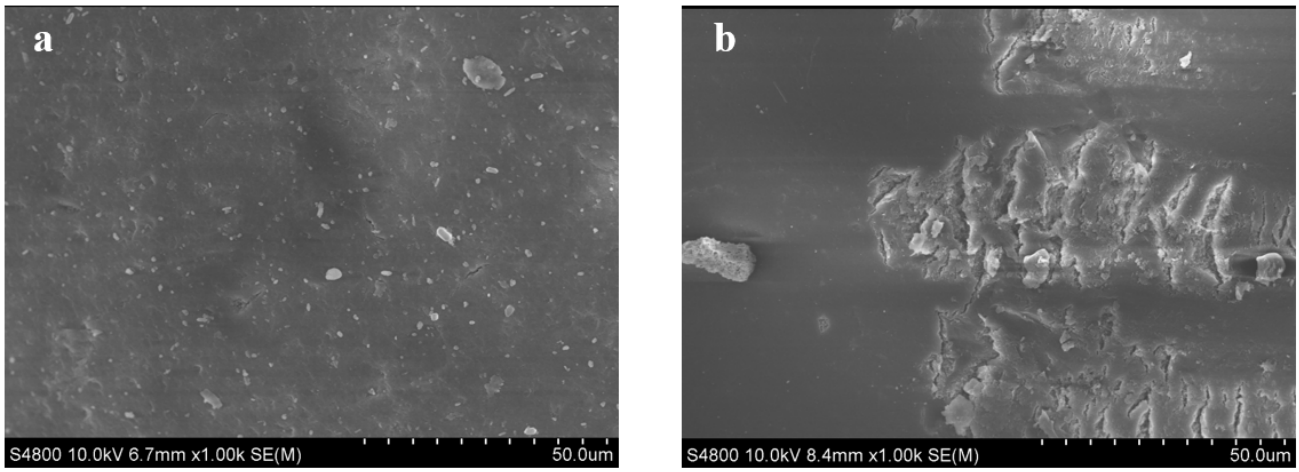

Figure 4. (**a**) SEM images of PS−Cl and (**b**) PS−DEA−5.

2.2. Adsorption Experiments

2.2.1. Adsorption Capacity

The adsorption performance of the obtained PS−DEA−x towards CPCA was determined through static adsorption experiments, as shown in Figure 5. Compared with raw PS−Cl, the adsorption capacity of PS−DEA−x to CPCA was increased, and the order was PS−DEA−5 > PS−DEA−7 > PS−DEA−3 > PS−DEA−1 > PS−DEA−0.5 > PS−Cl. The adsorption capacity was elevated with the increase in DEA. The reason for this phenomenon was that the amine groups in the resin could interact with the CPCA via electrostatic interaction and hydrogen bonding [11,31]. The carboxyl of CPCA and the amine on the PS−DEA−x play key roles in the adsorption process [32]. Therefore, PS−DEA−5 with more amine functional groups had a higher adsorption capacity for CPCA. However, it can be noted that the adsorption capacity of PS−DEA−5 was almost the same as that of PS−DEA−7. Combined with the characterization analysis, this was attributed to the similar loading amount of DEA in the adsorbent (Table 1) and a near−saturated loading quantity of DEA on PS−DEA−7, resulting in almost no increase in the adsorption capacity of PS−DEA−7 relative to PS−DEA−5. Based on the above observations, PS−DEA−5 was employed as a representative sample for the adsorption of CPCA in further adsorption investigations.

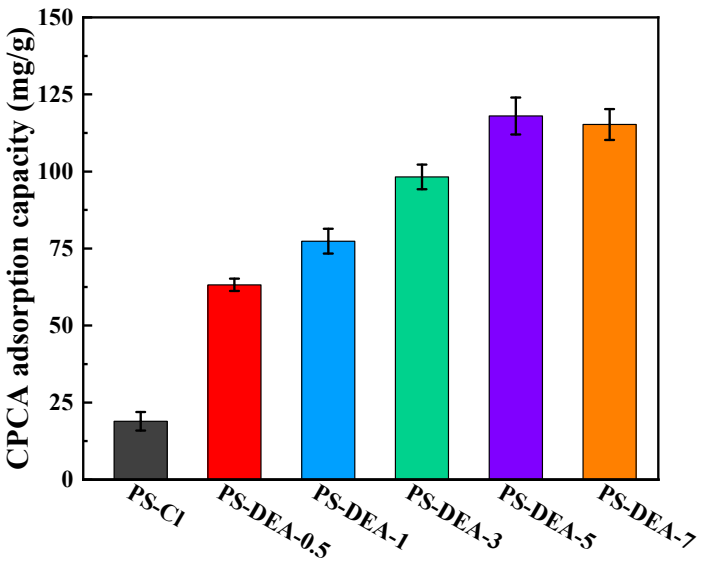

Figure 5. Adsorption capacity of PS−DEA−x on CPCA.

2.2.2. Adsorption Isotherms and Thermodynamics

As described in Figure 6, for the purpose of researching the effect of different initial concentrations on the CPCA adsorption, the Langmuir and Freundlich models were applied to fit the isotherm data. It is obvious that the adsorption capacity increases rapidly with the adsorbate concentration at the initial stage and then slows down because the adsorption sites tend to be saturated [33]. As expressed in Table 3, the Langmuir model was more suitable for describing the CPCA adsorption due to its high correlation coefficients ($R^2 > 0.99$), implying that monolayer adsorption occurred during CPCA adsorption on PS−DEA−5 [34]. In addition, the adsorption quantity of CPCA increased with temperature, indicating an endothermic adsorption process [35]. Based on the data from Table 3, the maximum adsorption capacity (207.2 mg/g) of the CPCA adsorption on PS−DEA−5 was predicted by the Langmuir model. Table 4 presents the calculation results of adsorption thermodynamic parameters, where it can be seen that the adsorption enthalpy change was positive, further confirming the deduction of the endothermic adsorption process. Furthermore, the negative value of ΔG reflected the spontaneous adsorption of CPCA onto PS−DEA−5. Meanwhile, positive values of ΔS mean that the disorder degree of solid–liquid interface increases when CPCA is adsorbed on the active site of the PS−DEA−5 and also reflect the high affinity of PS−DEA−5 to CPCA [36].

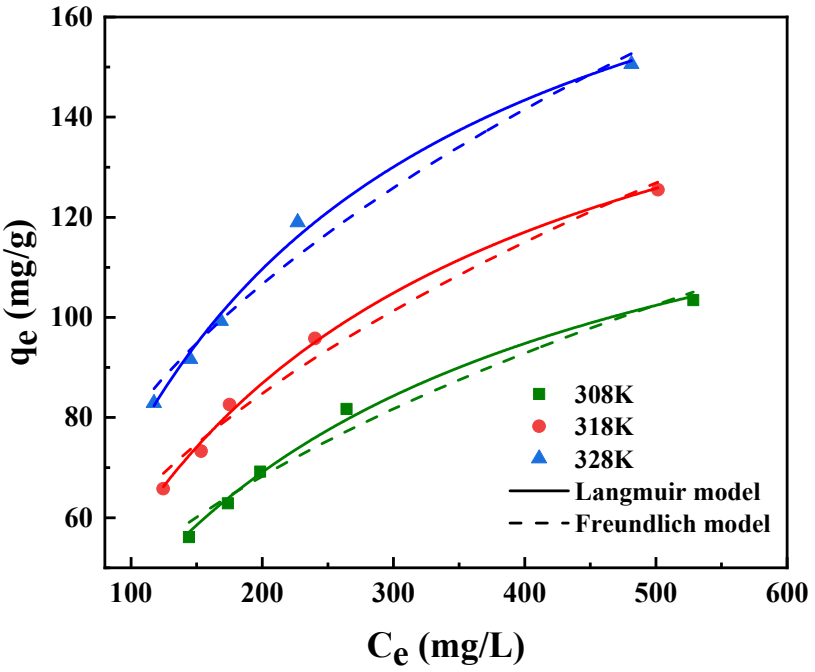

Figure 6. Adsorption thermodynamics for CPCA of PS−DEA−5 at different temperatures.

Table 3. Adsorption isotherms parameters of CPCA on PS−DEA−5.

Sample	Temperature (K)	Langmuir Model			Freundlich Model		
		q_m (mg/g)	k_L (L/mg)	R^2	n	k_F ((mg/g)·(L/mg)1/n)	R^2
PS−DEA−5	308	150.9	0.42×10^{-2}	0.994	0.40	6.51	0.979
	318	179.4	0.47×10^{-2}	0.996	0.44	8.25	0.976
	328	207.2	0.56×10^{-2}	0.995	0.44	12.23	0.979

Table 4. Thermodynamic parameters of CPCA adsorption on PS−DEA−5.

NAs	Temperature(K)	Δ*G* (kJ/mol)	Δ*H* (kJ/mol)	Δ*S* (J/(K·mol))
CPCA	308	−14.80	22.80	122.10
	318	−16.02		
	328	−17.24		

2.2.3. Adsorption Kinetics

To illustrate the adsorption behavior of PS−DEA−x towards CPCA, two kinetic models of pseudo−first−order and pseudo−second−order kinetic models were carried out. The fitting curve is shown in Figure 7, and the corresponding parameters are summarized in Table 5. The adsorption equilibrium of CPCA was reached in about 150 min, and the adsorption rate decreased substantially when the adsorption time exceeded 150 min, while the adsorption capacity only slightly increased. The fast adsorption of CPCA could be attributed to the existence of a large number of active sites and accessible diffusion pathways in PS−DEA−5, providing a strong driving force for the CPCA molecular transportation from oil phase to the surface of PS−DEA−5. As the contact time increased, more and more active adsorption sites were occupied, the adsorption process reached a plateau, and the adsorption rates were limited by the larger diffusion resistance [37]. As presented in Table 5, the much higher correlation coefficients ($R^2 \geq 0.99$) by the pseudo−second−order rate equation illustrated that chemical adsorption predominated the adsorption process. Noticeably, the correlation coefficient R^2 of the pseudo−first−order model was also as high as 0.97, which hinted that the physical adsorption should also give an outstanding contribution to the adsorption process [38]. Significantly, the K_2 value of PS−DEA−x increased gradually as the amine contents increased, which further reflected that the existence of amine played a predominant role in the adsorption performance of CPCA. This can be explained by the relatively strong interaction between CPCA and amine groups and therefore enhances the adsorption capacity.

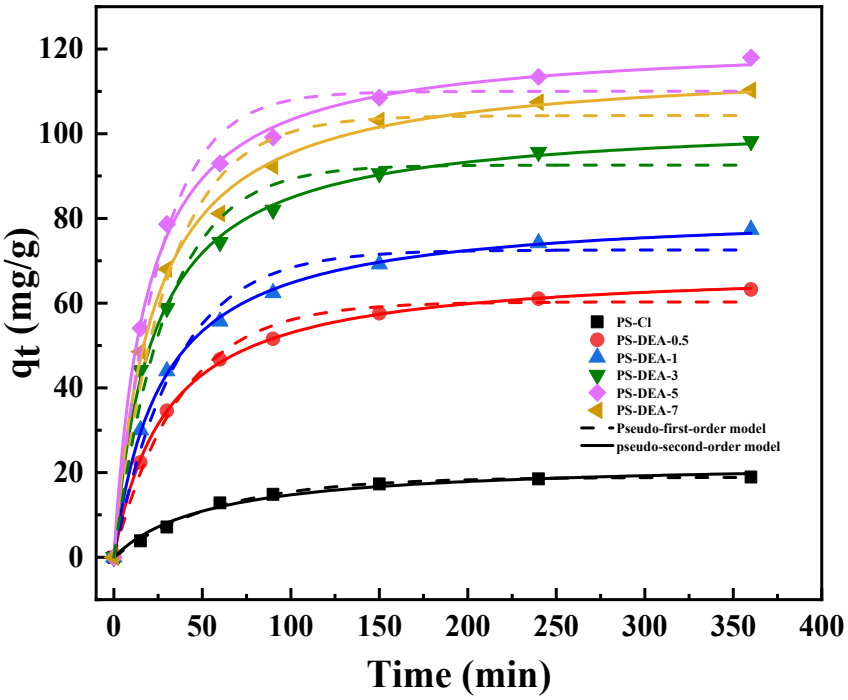

Figure 7. Adsorption kinetic fitting of pseudo−first−order and pseudo−second−order model on PS−DEA−x.

Table 5. Adsorption kinetic parameters of pseudo−first−order and pseudo−second−order model on PS−DEA−x.

Samples	Pseudo−First−Order Model			Pseudo−Second−Order Model		
	$q_{e,\ cal}$ (mg/g)	K_1 (1/min)	R^2	$q_{e,\ cal}$ (mg/g)	K_2 (g/(mg·min))	R^2
PS−Cl	18.9	0.017	0.997	22.8	2.09×10^{-4}	0.986
PS−DEA−0.5	60.3	0.027	0.990	68.8	3.83×10^{-4}	0.993
PS−DEA−1	72.6	0.029	0.980	82.2	4.37×10^{-4}	0.994
PS−DEA−3	92.6	0.033	0.978	103.6	4.46×10^{-4}	0.996
PS−DEA−5	110.0	0.040	0.981	122.2	4.89×10^{-4}	0.998
PS−DEA−7	104.3	0.033	0.976	116.7	4.50×10^{-4}	0.997

2.2.4. Dynamic Adsorption

Dynamic adsorption is a direct evaluation of an adsorbent's efficacy during continuous column operation; hence, the breakthrough characteristics of PS−DEA−5 towards CPCA were tested in a fixed−bed experiment. Figure 8 shows the breakthrough curves of CPCA adsorption on PS−DEA−5 at 328 K in an adsorption column with diameter of 6 mm and height of 6.7 cm. When transformer oil (TAN = 0.15 mg KOH/g) was pumped into the adsorption column filled with 1 g of PS−DEA−5, it would reach the adsorption equilibrium at about 1000 min. As shown in Table 6, the breakthrough curve was fitted to the Thomas model, which is developed on the basis of Langmuir kinetics, and the axial dispersion in adsorption column is assumed to be negligible [39]. Figure 8 and Table 6 also show that the Thomas model could better describe the whole adsorption process as the coefficient constant R^2 was as high as 0.995. This indicates that the limiting step was not caused by external and internal diffusion [40]. Additionally, the maximal adsorption capacity of CPCA predicted by the Thomas model was 187.5 mg/g. After all, it can be calculated that 1 g of PS−DEA−5 can decontaminate about 1050 mL transformer oil (TAN = 0.15 mg KOH/g), and about 760 mL transformer oil can be reduced to less than 0.1 of the TAN, which was eligible for reuse.

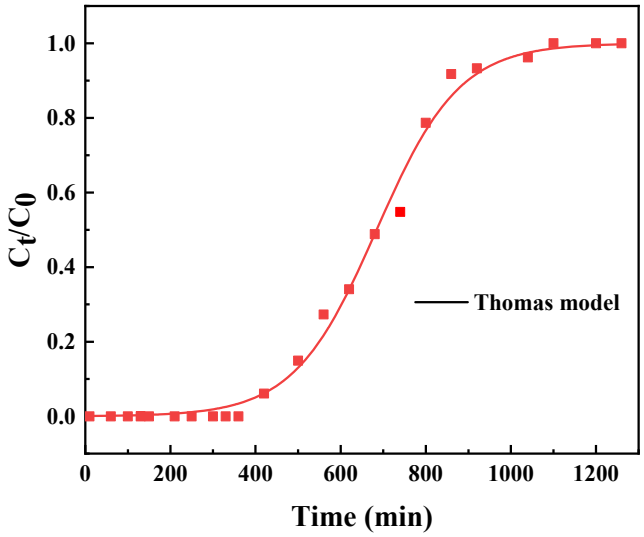

Figure 8. Dynamic adsorption curve of CPCA on PS−DEA−5.

Table 6. Thomas model fitting parameters.

C_0 (mg/L)	Q (mL/min)	Thomas Model Parameters			
		K_{Th} (L/(h·mg))	$q_{bed,Th}$ (mg/g)	M (g)	R^2
274	1.0	0.00325	187.5	1.0	0.995

3. Experimental Methods

3.1. Materials and Reagents

Chloromethyl polystyrene resin (PS−Cl, cross−linking degree 8%, Cl content 18%) was bought from Nankai Chemical University Factory (Tianjin, Chain), N, N−dimethyl formamide (DMF), ethyl alcohol, alkali blue 6B, cyclopentane carboxylic acid (CPCA) and diethylamine (DEA) were all supplied by Aladdin Reagent (Shanghai, China) Co., Ltd. Potassium hydroxide was bought from Sinopharm Chemical Reagent (Shanghai, Chain) Co., Ltd. Transformer oil was provided by Moroke (Shanghai, Chain) Co., Ltd.

3.2. Synthesis of Adsorbent

The synthesis route of DEA−modified PS−Cl is shown in Scheme 1. About 5.0 g of PS−Cl beads and 50 mL DMF were mixed in a flask to be swollen for approximately 12 h. Afterwards, various amounts of DEA were added to the above mixture, depending on the molar ratios of DEA to chloromethyl, i.e., 0.5, 1, 3, 5, and 7, respectively. The reaction mixture was stirred at 343 K for 10 h, washed thoroughly with ethyl alcohol and deionized water, and finally dried at 323 K for 6 h in a vacuum oven. The prepared samples were notated PS−DEA−x, where x represented the molar ratios of DEA to chloromethyl.

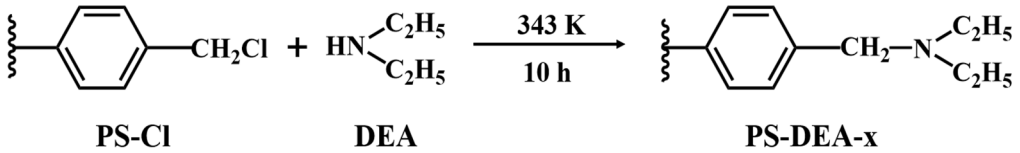

Scheme 1. Synthesis of PS−DEA−x.

3.3. Preparation of Simulated Oil

The total acid number (TAN) is considered the index to predict the corrosiveness ability of the naphthenic acids. TAN (mg KOH/g) values exceeding 0.1 indicate that the oil or any petroleum fractions may cause damage to equipment material. Therefore, the model transformer oils were prepared aiming TAN around 0.15 mg KOH/g, as shown in the following expression:

$$m_{NA} = TAN \frac{M_{NA}}{M_{KOH}} \rho_{oil} V_{oil} \quad (1)$$

where m_{NA} (g) is the mass of acid used to prepare a certain volume V_{oil} (mL) of a known *TAN* value solution; ρ_{oil} (g/mL) and M_{NA} (g/mol) are the specific mass and the molecular mass of the CPCA, respectively; M_{KOH} (mg/mol) is the molecular mass of the KOH.

3.4. Characterization

The organic groups of the resin were determined by Fourier transform infrared spectroscopy (FTIR, ThemoNicolet IS 50 IR spectrometer, Waltham, MA, USA). The quantitative analysis of carbon, hydrogen, nitrogen, and other elements was analyzed with an elemental analyzer (EA, Vario EL cube, Hanau, Germany). The stability test was performed using a thermogravimetric analyzer (Mettler Toledo TGA/DSC 3+). N_2 adsorption–desorption experiments of all samples were tested on the Micrometrics system (Micromeritics 3 Flex Instrument, Norcross, GA, USA). The specific surface area of the samples was calculated through the Brunauer–Emmett–Teller (BET) model and the calculation of t−plot micropore volume, while the pore size distribution and total pore volume were determined by the BJH method to the nitrogen desorption data. Scanning electron microscopy (SEM) images of all samples were acquired using an S−4800N field emission microscope (Hitachi, Tokyo, Japan).

3.5. Adsorption Experiments

3.5.1. Adsorption Capacity

CPCA was dissolved into transformer oil and 0.15 mg KOH/g simulated waste transformer oil was accurately prepared. In all, 10 mg of adsorbent was mixed with 10 g of the simulated waste transformer oil and shaken in a thermostatic oscillating water bath at 328 K with an oscillation frequency of 140 r/min. After 6 h of adsorption, 5 g of the oil was taken for titration with alcoholic potassium hydroxide to determine the acid value. The adsorption capacity (q_e) was computed by the following equation.

$$C = TAN\frac{M_{NA}}{M_{KOH}}\rho_{oil} \tag{2}$$

$$q_e = \frac{(C_0 - C_e)\cdot V}{m} \tag{3}$$

where C_0 (mg/L) and C_e (mg/L) represent the initial concentration and equilibrium concentration, respectively, while V (L) and m (g) represent the volume of the aqueous solution and the mass of adsorbent, respectively.

3.5.2. Adsorption Kinetics

The adsorption kinetics experiments were implemented at 328 K, and the initial acid value of the oil was 0.15 mg KOH/g. For each kinetic experiment, simulated oil and adsorbent were simultaneously weighed into six 500 mL flasks with the same oil/adsorbent mass ratio (1000:1) in each flask. The flasks were shaken at 328 K for 6 h. In this process, a flask was taken every 10 to 30 min to separate the adsorbent from the oil, and the oil sample was taken for titration with alcoholic potassium hydroxide to determine the acid value. The adsorption quantity at time t (min), q_t (mg/g), was calculated using Equations (2) and (3).

The adsorption kinetics were investigated using the pseudo−first−order kinetic model and pseudo−second−order kinetic model. The expressions for kinetic models are as follows:

Pseudo−first−order [41]:

$$\lg(q_e - q_t) = \lg q_e - \frac{k_1\cdot t}{\ln 10} \tag{4}$$

$$q_t = q_{e,exp} - \frac{q_{e,exp}}{e^{k_1\cdot t}} \tag{5}$$

Pseudo−second−order [41]:

$$\frac{t}{q_t} = \frac{1}{k_2\cdot q_e^2} + \frac{t}{q_e} \tag{6}$$

$$q_t = \frac{t\cdot k_2\cdot q_{e,exp}^2}{1 + t\cdot k_2\cdot q_e} \tag{7}$$

where q_t (mg/g), $q_{e,\,exp}$ (mg/g) are the adsorption capacity at time t (min) and equilibrium, respectively. k_1 (1/min), k_2 (g/(mg·min)) are rate constants for pseudo−first−order and pseudo−second−order models.

3.5.3. Adsorption Isotherms and Thermodynamics

Adsorption isotherm experiments were performed by adding 15 mg resins into a series of flasks containing various initial acid value (0.10, 0.13, 0.15, 0.19 and 0.40 mg KOH/g) of 15 g of simulated oil. After shaking at 308, 318, and 328 K for 6 h the absorbent was separated from the oil. Finally, the adsorption capacity at time t, q_t (mg/g), was calculated using Equations (2) and (3).

The adsorption isotherms were fitted by Langmuir and Freundlich models. The model equations are as follows:

Langmuir:

$$q_e = \frac{q_m \cdot k_L \cdot c_e}{1 + k_L \cdot c_e} \tag{8}$$

Freundlich:

$$q_e = k_F \cdot c_e^{\frac{1}{n}} \tag{9}$$

where q_e (mg/g), q_m (mg/g) represent the equilibrium adsorption capacity and maximum adsorption capacity, respectively. c_e (mg/L) is the equilibrium concentration of CPCA, while k_L (L/mg), k_F ((mg/g)·(L/mg)$^{1/n}$) are the Langmuir constant and Freundlich adsorption constant, respectively. n is a measure of adsorption intensity.

Adsorption thermodynamics:

$$k_{qc} = \frac{q_e}{c_e} \tag{10}$$

$$\Delta G = -RT \cdot \ln K_c \tag{11}$$

$$\Delta G = \Delta H - T\Delta S \tag{12}$$

$$ln(\rho k_{qc}) = -\frac{\Delta H}{RT} + \frac{\Delta S}{R} \tag{13}$$

where K_c is the equilibrium constant and k_{qc} (L/g) is the equilibrium adsorption coefficient. q_e (mg/g), C_e (mg/L) are the reduced mass concentration and equilibrium concentration of the solution after adsorption, respectively. R J/(mol·K) is the universal gas constant, and T (K) represents the solution temperature. ΔG (kJ/mol) is the change in Gibbs free energy; ΔH (kJ/mol) is the enthalpy; ΔS (J/(mol·K)) is the entropy.

3.5.4. Dynamic Adsorption

For dynamic resin adsorption, the adsorption column was a glass column (diameter 10 mm) filled with 1 g dry resin. The adsorption column temperature was 328 K, which remained constant during the adsorption process. The simulated oil with an initial acid value of 0.15 mg KOH/g was passed through the resin column at flow rates of 1.0 mL/min, and the acid value of the exported oil was continuously recorded until the initial acid value was reached. Dynamic adsorption capacity was calculated by numerical integration of Equations (2) and (14).

$$q_t = \frac{QC_0t - Q\int_0^t C_t dt}{m} \tag{14}$$

where t (min)is the time at any time; C_t (mg/L) is the concentration of outlet liquid at any time; C_0 (mg/L) is the concentration of inlet liquid; Q (mL/min) is the volume flow rate of liquid; q_t (mg/g) is the dynamic equilibrium adsorption capacity. m (mg) is the mass of adsorbent in the adsorption column.

4. Conclusions

In this work, we synthesized a kind of amine−modified resin (PS−DEA−x) to improve the adsorption capacity to NAs. The static adsorption capacity of PS−DEA−5 was 110.0 mg/g, which was about five times higher than that of unmodified PS−Cl. The adsorption isotherms were well consistent with the Langmuir model, and the adsorption kinetics was in good agreement with the pseudo−second−order model. At an initial TAN of 0.15 mg KOH/g and a flow rate of 1.0 mL/min, the breakthrough capacity of CPCA on PS−DEA−5 was 187.5 mg/g, and about 760 mL of transformer oil can meet reuse standards. After adsorption, PS−DEA−x are easy to separate from the transformer oil and will not affect the insulation performance of the transformer oil. Based on the above results, this study indicates that amine resin may be promising in the removal of NAs from transformer oil.

Author Contributions: Y.W.: methodology, validation, investigation, writing—original draft, software. P.D.: writing—original draft, formal analysis. X.Y.: resources. Q.L.: conceptualization, supervision, funding acquisition, writing—review and editing. Z.F.: funding acquisition. X.C.: data curation. Z.Z.: data curation. J.T.: funding acquisition. M.C.: funding acquisition. X.Q.: supervision, writing—review and editing, funding acquisition. All authors have read and agreed to the published version of the manuscript.

Funding: This study was supported by Province Key R&D Program of Jiangsu (BE2019735), National Key Research and Development Program (2019YFC1905804, 2017YFC0210903, 2017YFB0307304), Project '333' of Jiangsu Province (BRA2016418), State Key Laboratory of Materials−Oriented Chemical Engineering (ZK201610), and the Priority Academic Program Development of Jiangsu Higher Education Institutions (PAPD).

Institutional Review Board Statement: Not applicable.

Informed Consent Statement: Not applicable.

Data Availability Statement: Not applicable.

Conflicts of Interest: The authors declare no conflict of interest.

References

1. Safiddine, L.; Hadj−Ziane Zafour, A.; Fofana, I.; Skender, A.; Guerbas, F.; Boucherit, A. Transformer oil reclamation by combining several strategies enhanced by the use of four adsorbents. *IET Gener. Transm. Distrib.* **2017**, *11*, 2912–2920. [CrossRef]
2. Abdi, S.; Boubakeur, A.; Haddad, A.; Harid, N. Influence of artificial thermal aging on transformer oil properties. *Electr. Power Compon. Syst.* **2011**, *39*, 1701–1711. [CrossRef]
3. Bayrak, Y. Application of Langmuir isotherm to saturated fatty acid adsorption. *Microporous Mesoporous Mater.* **2006**, *87*, 203–206. [CrossRef]
4. Silva, J.P.; Costa, A.L.H.; Chiaro, S.S.X.; Delgado, B.E.P.C.; de Figueiredo, M.A.G.; Senna, L.F. Carboxylic acid removal from model petroleum fractions by a commercial clay adsorbent. *Fuel Process. Technol.* **2013**, *112*, 57–63. [CrossRef]
5. Vaz, B.G.; Abdelnur, P.V.; Rocha, W.F.C.; Gomes, A.O.; Pereira, R.C.L. Predictive Petroleomics: Measurement of the total acid number by electrospray fourier transform mass spectrometry and chemometric analysis. *Sustain. Energy Fuels* **2013**, *27*, 1873–1880. [CrossRef]
6. Qian, Y.−H.; Su, W.; Huang, Y.−B.; Zhong, Z.−s. Influence of hydrogenated transformer oil on construction materials inside transformer. *IEEE Trans. Electr. Insul.* **2015**, *22*, 1588–1593. [CrossRef]
7. Moghaddam, J.; Sarrafmamoory, R.; Abdollahy, M.; Yamini, Y. Purification of zinc ammoniacal leaching solution by cementation: Determination of optimum process conditions with experimental design by Taguchi's method. *Sep. Purif. Technol.* **2006**, *51*, 157–164. [CrossRef]
8. Jafari, A.J.; Hassanpour, M. Analysis and comparison of used lubricants, regenerative technologies in the world. *Resour Conserv Recycl* **2015**, *103*, 179–191. [CrossRef]
9. Taiwo, E.A.; Bello, T. Hydro−distillation of spent lubricating oil and characterization of the product. *Petrol Sci. Technol.* **2019**, *38*, 345–353. [CrossRef]
10. Hendges, L.T.; Costa, T.C.; Temochko, B.; Gómez González, S.Y.; Mazur, L.P.; Marinho, B.A.; da Silva, A.; Weschenfelder, S.E.; de Souza, A.A.U.; de Souza, S.M.A.G.U. Adsorption and desorption of water−soluble naphthenic acid in simulated offshore oilfield produced water. *Process Saf. Environ. Prot.* **2021**, *145*, 262–272. [CrossRef]
11. Niasar, H.S.; Li, H.; Kasanneni, T.V.R.; Ray, M.B.; Xu, C. Surface amination of activated carbon and petroleum coke for the removal of naphthenic acids and treatment of oil sands process−affected water (OSPW). *Chem. Eng. J.* **2016**, *293*, 189–199. [CrossRef]
12. Simonsen, G.; Strand, M.; Norrman, J.; Øye, G. Amino−functionalized iron oxide nanoparticles designed for adsorption of naphthenic acids. *Colloids Surf. A Physicochem. Eng. Asp.* **2019**, *568*, 147–156. [CrossRef]
13. Wu, C.; De Visscher, A.; Gates, I.D. On naphthenic acids removal from crude oil and oil sands process−affected water. *Fuel* **2019**, *253*, 1229–1246. [CrossRef]
14. Barros, E.V.; Filgueiras, P.R.; Lacerda, V.; Rodgers, R.P.; Romão, W. Characterization of naphthenic acids in crude oil samples—A literature review. *Fuel* **2022**, *319*, 123775. [CrossRef]
15. Gaikar, V.G.; Maiti, D. Adsorptive recovery of naphthenic acids using ion−exchange resins. *React Funct. Polym.* **1996**, *31*, 155–164. [CrossRef]
16. Zhou, F.; Man, R.; Huang, J. Hyper−cross−linked polymers functionalized with primary amine and its efficient adsorption of salicylic acid from aqueous solution. *J. Chem. Thermodyn.* **2019**, *131*, 387–392. [CrossRef]
17. Niasar, H.S.; Li, H.; Das, S.; Kasanneni, T.V.R.; Ray, M.B.; Xu, C.C. Preparation of activated petroleum coke for removal of naphthenic acids model compounds: Box−Behnken design optimization of KOH activation process. *J. Environ. Manag.* **2018**, *211*, 63–72. [CrossRef]

18. Xiang, Y.; Liu, Y.; Li, M.; Bai, W.; Liu, G.; Xu, L. The recovery of Au(III) by hydrogel−like beads. *Hydrometallurgy* **2023**, *215*, 105964. [CrossRef]
19. Kim, J.; Oh, S.; Kwak, S.-Y. Magnetically separable magnetite–lithium manganese oxide nanocomposites as reusable lithium adsorbents in aqueous lithium resources. *Chem. Eng. J.* **2015**, *281*, 541–548. [CrossRef]
20. Xiong, C.; Zheng, Y.; Feng, Y.; Yao, C.; Ma, C.; Zheng, X.; Jiang, J. Preparation of a novel chloromethylated polystyrene−2−amino−1,3,4−thiadiazole chelating resin and its adsorption properties and mechanism for separation and recovery of Pt(IV) from aqueous solutions. *J. Mater. Chem. A* **2014**, *2*, 5379–5386. [CrossRef]
21. Ramsdale-Capper, R.; Foreman, J.P. Internal antiplasticisation in highly crosslinked amine cured multifunctional epoxy resins. *Polymer* **2018**, *146*, 321–330. [CrossRef]
22. Ye, F.; Yang, R.; Hua, X.; Zhao, G. Adsorption characteristics of rebaudioside A and stevioside on cross-linked poly(styrene−co−divinylbenzene) macroporous resins functionalized with chloromethyl, amino and phenylboronic acid groups. *Food Chem.* **2014**, *159*, 38–46. [CrossRef] [PubMed]
23. Wang, X.; Deng, R.; Jin, X.; Huang, J. Gallic acid modified hyper-cross-linked resin and its adsorption equilibria and kinetics toward salicylic acid from aqueous solution. *Chem. Eng. J.* **2012**, *191*, 195–201. [CrossRef]
24. Liu, Y.; Di, D.; Bai, Q.; Li, J.; Chen, Z.; Lou, S.; Ye, H. Preparative separation and purification of rebaudioside a from steviol glycosides using mixed-mode macroporous adsorption resins. *J. Agric. Educ. Ext.* **2011**, *59*, 9629–9636. [CrossRef] [PubMed]
25. Kuang, W.; Li, H.; Huang, J.; Liu, Y.-N. Tunable porosity and polarity of the polar hyper−cross−linked resins and the enhanced adsorption toward phenol. *Ind. Eng. Chem. Res.* **2016**, *55*, 12213–12221. [CrossRef]
26. Huang, J.; Deng, R.; Huang, K. Equilibria and kinetics of phenol adsorption on a toluene−modified hyper−cross−linked poly(styrene−co−divinylbenzene) resin. *Chem. Eng. J.* **2011**, *171*, 951–957. [CrossRef]
27. Zhang, Y.; Chen, Y.; Wang, C.; Wei, Y. Immobilization of 5−aminopyridine−2−tetrazole on cross−linked polystyrene for the preparation of a new adsorbent to remove heavy metal ions from aqueous solution. *J. Hazard. Mater.* **2014**, *276*, 129–137. [CrossRef]
28. Zhuo, W.; Xu, H.; Huang, R.; Zhou, J.; Tong, Z.; Xie, H.; Zhang, X. A chelating polymer resin: Synthesis, characterization, adsorption and desorption performance for removal of Hg(II) from aqueous solution. *J. Iran. Chem. Soc.* **2017**, *14*, 2557–2566. [CrossRef]
29. Wang, H.; Wang, Y.; Sun, X.; Hu, H.; Peng, Q. Two functional post−cross−linked polystyrene resins: Effect of structure on the enhanced removal of benzene sulfonic acid. *Colloids Surf. A Physicochem. Eng. Asp.* **2020**, *588*, 124398. [CrossRef]
30. Wei, M.; Yu, Q.; Mu, T.; Hou, L.; Zuo, Z.; Peng, J. Preparation and characterization of waste ion−exchange resin−based activated carbon for CO_2 capture. *Adsorption* **2016**, *22*, 385–396. [CrossRef]
31. Ling, C.; Li, X.; Zhang, Z.; Liu, F.; Deng, Y.; Zhang, X.; Li, A.; He, L.; Xing, B. High Adsorption of sulfamethoxazole by an amine−modified polystyrene−divinylbenzene resin and its mechanistic insight. *Crit Rev. Environ. Sci. Technol.* **2016**, *50*, 10015–10023. [CrossRef]
32. Jayalath, S.; Larsen, S.C.; Grassian, V.H. Surface adsorption of nordic aquatic fulvic acid on amine−functionalized and non−functionalized mesoporous silica nanoparticles. *Environ. Sci. Nano* **2018**, *5*, 2162–2171. [CrossRef]
33. Sun, Y.; Gu, Y.; Yang, J. Adsorption of N−heterocyclic compounds from aqueous solutions by sulfonic acid−functionalized hypercrosslinked resins in batch experiments. *Chem. Eng. J.* **2022**, *428*, 131163. [CrossRef]
34. Wang, R.; Zou, H.; Zheng, R.; Feng, X.; Xu, J.; Shangguan, Y.; Luo, S.; Wei, W.; Yang, D.; Luo, W.; et al. Molecular Dynamics beyond the monolayer adsorption as derived from Langmuir curve fitting. *Inorg. Chem.* **2022**, *61*, 7804–7812. [CrossRef]
35. Zheng, Y.; Xiong, C.; Yao, C.; Ye, F.; Jiang, J.; Zheng, X.; Zheng, Q. Adsorption performance and mechanism for removal of Cd(II) from aqueous solutions by D001 cation−exchange resin. *Water Sci. Technol.* **2014**, *69*, 833–839. [CrossRef]
36. Luo, P.; Zhao, Y.; Zhang, B.; Liu, J.; Yang, Y.; Liu, J. Study on the adsorption of Neutral Red from aqueous solution onto halloysite nanotubes. *Water Res.* **2010**, *44*, 1489–1497. [CrossRef]
37. Yuan, W.; Zhou, L.; Zhang, Z.; Ying, Y.; Fan, W.; Chai, K.; Zhao, Z.; Tan, Z.; Shen, F.; Ji, H. Synergistic dual−functionalities of starch−grafted−styrene hydrophilic porous resin for efficiently removing bisphenols from wastewater. *Chem. Eng. J.* **2022**, *429*, 132350. [CrossRef]
38. Simonin, J.−P. On the comparison of pseudo−first order and pseudo−second order rate laws in the modeling of adsorption kinetics. *Chem. Eng. J.* **2016**, *300*, 254–263. [CrossRef]
39. Chu, K.H. Fixed bed sorption: Setting the record straight on the Bohart−Adams and Thomas models. *J. Hazard. Mater.* **2010**, *177*, 1006–1012. [CrossRef]
40. Li, M.; Tang, S.; Zhao, Z.; Meng, X.; Gao, F.; Jiang, S.; Chen, Y.; Feng, J.; Feng, C. A novel nanocomposite based silica gel/graphene oxide for the selective separation and recovery of palladium from a spent industrial catalyst. *Chem. Eng. J.* **2020**, *386*, 123947. [CrossRef]
41. Ni, Y.Y.; Yang, J.H.; Sun, L.X.; Liu, Q.; Fei, Z.Y.; Chen, X.; Zhang, Z.X.; Tang, J.H.; Cui, M.F.; Qiao, X. La/LaF_3 co−modified MIL−53(Cr) as an efficient adsorbent for the removal of tetracycline. *J. Hazard. Mater.* **2022**, *426*, 128112. [CrossRef] [PubMed]